Monofractal and multifractal analysis of the spatial distribution of earthquakes in the central zone of Chile

Denisse Pastén,[1] Víctor Muñoz,[1,2] Armando Cisternas,[3] José Rogan,[1,2] and Juan Alejandro Valdivia[1,2]
[1]*Departamento de Física, Facultad de Ciencias, Universidad de Chile, Casilla 653, Santiago, Chile*
[2]*Centro para el Desarrollo de la Nanociencia y la Nanotecnología (CEDENNA), Santiago, Chile*
[3]*Departamento de Geofísica, Facultad de Ciencias Físicas y Matemáticas, Universidad de Chile, Casilla 653, Santiago, Chile*
(Received 23 June 2011; published 27 December 2011)

Statistical and fractal properties of the spatial distribution of earthquakes in the central zone of Chile are studied. In particular, data are shown to behave according to the well-known Gutenberg-Richter law. The fractal structure is evident for epicenters, not for hypocenters. The multifractal spectrum is also determined, both for the spatial distribution of epicenters and hypocenters. For negative values of the index of multifractal measure q, the multifractal spectrum, which usually cannot be reliably found from data, is calculated from a generalized Cantor-set model, which fits the multifractal spectrum for $q > 0$, a technique which has been previously applied for analysis of solar wind data.

DOI: 10.1103/PhysRevE.84.066123 PACS number(s): 89.75.−k, 91.30.Dk, 05.45.Df

I. INTRODUCTION

Recently, there has been a growing interest in studying Earth's seismicity from the perspective of a complex system. Several analytical tools developed or used in the study of complexity, such as the calculation of fractal dimensions, event distributions, complex network analysis, etc., have been applied to the study of seismic activity [1–5].

Seismic activity is the result of the interaction between tectonic plates. Relative motion between them eventually leads to a buildup of stress, leading to an energy release in the form of seismic waves which propagate through Earth. It is thus natural to relate seismic activity to avalanches in sandpile models [6], where seisms can be regarded as the result of the Earth being in a self-organized critical state [7–10]. Evidence for this comes from the fact that the energy release distribution (avalanche size or seism magnitude) follows a power law in both cases, and that the spatial distribution (of avalanches or seisms) shows a fractal structure. Calculation of the fractal dimension of the earthquake spatial distribution in a given zone does not only give statistical information on past events, but has also been proposed as a prediction tool to find precursors of volcano eruptions, for instance [11].

In this regard, it is important to keep in mind that the study of seismicity has important practical consequences in terms of assessing risks for building policies, determining locations for human settlements, and, eventually, for saving human lives. One can take the approach of studying the detailed dynamics of a certain fault, for instance, in order to determine how stress is distributed, in an attempt to establish the risk of a major event in a particular zone. Another approach is to study a large number of seismic zones in order to gain insight about possible universal features of seismicity, which may be independent of the particular type of fault or soil involved, and of the recent history of the adjacent plates. Both approaches are complementary, and serve different purposes in the larger objective to understand seismicity.

In this paper we deal with the second approach, analyzing some statistical and fractal properties of seismic activity in the central zone of Chile, an area of strong seismicity but where few studies of these kind have been carried out, thus strengthening the point that seismicity does have universal qualitative and quantitative features. In particular, we find that data follow two well-established behaviors present in other seismic data, namely, the Gutenberg-Richter law, and the fact that the spatial distribution of seisms has a fractal structure.

Another well-established feature in seismic data is that the earthquake spatial distribution also exhibits a multifractal structure [12–14]. However, usually only the region of the multifractal spectrum corresponding to positive values of the index of multifractal measure q can be reliably obtained from earthquake data, due to experimental uncertainties. In this paper we use a generalized Cantor-set model [15,16] in order to first fit the multifractal spectrum for $q > 0$, and then extend it for negative values of q, a technique which has been previously used for the analysis of solar wind data [17].

Thus, the purpose of this paper is to study the fractal characteristics of the earthquake spatial distribution in the central zone of Chile, corresponding to events occurring in the Nazca subduction zone. First, in Sec. II, the main features of the dataset we used for the analysis are discussed. In Sec. III, event magnitudes are shown to follow the well-known Gutenberg-Richter power-law distribution [18]. Then, in Sec. IV, the spatial distribution of earthquakes is shown to have a fractal structure, and the box-counting dimension is calculated, both for epicenters and for hypocenters. In Sec. V, the multifractal distribution of epicenters and hypocenters is studied. In Sec. VI the multifractal spectrum for $q < 0$ is found by using a generalized Cantor-set model. Finally, in Sec. VII results are summarized and discussed.

II. EARTHQUAKE DATA

The data used for this paper have been provided by the Chilean Servicio Sismológico Nacional (National Seismologic Service) [19]. They correspond to over 17 000 seismic events of magnitude higher that 1.6 recorded between October 2000 and January 2007, and between latitudes 29° S and 35.5° S, and between longitudes 69.501° W and 73.944° W (central zone of Chile), contained within a volume $L_{\mathrm{NS}} = 730$ km long in

the North-South direction, $L_{\mathrm{EW}} = 500$ km in the East-West direction, and $L_z = 700$ km in depth.

The data provide the position of the seismic event (hypocenter), the time of the event, and the local or Richter magnitude [20], which is related to the amplitude of the seismic wave and to the energy release:

$$M_L = \log_{10}(A) - \log_{10}(A_0)\delta, \tag{1}$$

where δ is the distance from the epicenter, A is the amplitude of the S waves at 600 km from the epicenter, and A_0 is a standard value, which depends on the time delay between the P wave and the S wave at the monitoring station.

III. GUTENBERG-RICHTER LAW

One of the few universal laws regarding earthquakes is the Gutenberg-Richter law [18], which states that $N(M_L)$, the number of earthquakes of magnitude larger than M_L, is related to M_L by

$$\ln[N(M_L)] = a + bM_L,$$

where a and b are constants. Since the local magnitude is related to the logarithm of the energy released, it follows that the Gutenberg-Richter law simply states that the distribution of earthquakes as a function of energy is a power law, just as avalanches in a sandpile model [6].

Figure 1 shows the distribution of events as a function of local magnitude. The data do in fact follow a linear relation for large magnitudes, with slope $b = -0.901 \pm 0.022$ (error calculated using the least-squares technique), thus showing that the Gutenberg-Richter law is satisfied by the data. This is consistent with many other similar studies for various sets of data in different seismic zones.

Figure 1 also implies that there is no characteristic magnitude in seismic activity, a scale-free property which is closely related to fractality, a feature which our data also have, as we will show in the next section.

IV. MONOFRACTAL ANALYSIS

In order to establish the self-similar properties of the data, we study the earthquake spatial distribution of epicenters

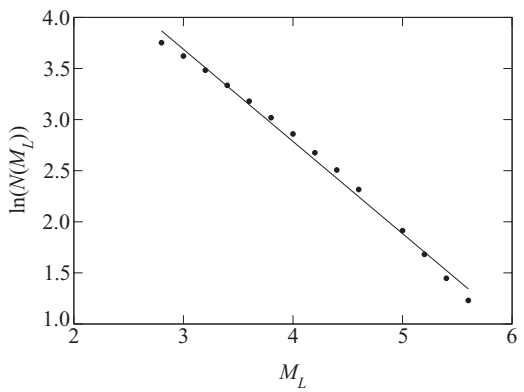

FIG. 1. Distribution function of seismic events as a function of local magnitude. Dots: data; line: linear fit.

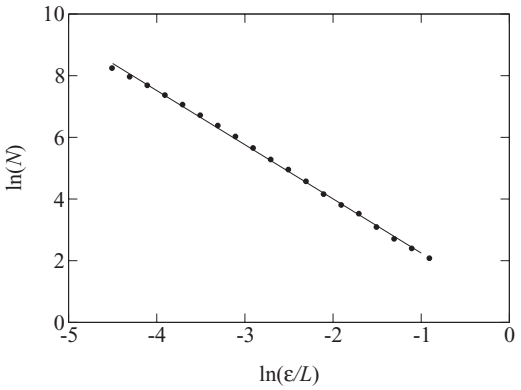

FIG. 2. Log-log plot of the number of boxes containing earthquake epicenters vs normalized box side ε/L_e. A linear scaling, consistent with Eq. (2), is present. The slope corresponds to the box-counting dimension $D_0 = 1.73$.

and hypocenters, and calculate its box-counting dimension [21–24].

In the case of epicenters, we divide the rectangular zone of area $L_{\mathrm{NS}} \times L_{\mathrm{EW}}$ in squares of side ε, and count the number of squares $N(\varepsilon)$ which contain data. For small ε,

$$N(\varepsilon) \simeq \varepsilon^{-D_0}, \tag{2}$$

where D_0 is the box-counting dimension.

Figure 2 shows that our data indeed follow the scaling Eq. (2) for epicenters. A similar plot is also obtained for hypocenters. In order to calculate the logarithm of an adimensional quantity for the abscissas, the box side is normalized by the square root of the total area $L_e = \sqrt{L_{\mathrm{NS}} L_{\mathrm{EW}}}$ for the case of epicenters, and it is normalized by the cubic root of the total volume $L_h = \sqrt[3]{L_{\mathrm{NS}} L_{\mathrm{EW}} L_z}$ for the case of hypocenters.

The resulting box-counting dimensions are

$$D_0^{(\mathrm{epi})} = 1.73 \pm 0.02,$$
$$D_0^{(\mathrm{hypo})} = 2.02 \pm 0.05,$$

respectively, where the error is calculated from the least-square fit of $\ln N$ vs $\ln \epsilon$.

It is interesting to note that these values are similar to the fractal dimensions calculated for other seismic zones [13,21,22,25], and in fact approximately correspond to the observed values for rocky soils, which matches the type of soil in the zone studied [26].

Table I shows a comparison of the values of D_0 and b for the Chilean data studied in this paper, and data for other seismic zones.

Also notice that the fractal structure of the data is much more evident for epicenters. However, the fact that the fractal dimension for hypocenters is approximately equal to 2 is also consistent with previous results, suggesting that faults can be modeled by a percolation model, with seisms only occurring at the active part of the fault, leading to a low dimensionality for hypocenter data [28,29].

It is also interesting to note that typical values of b range between $0.8 < b < 1.2$, depending on the tectonics of the region [26,30], and our results fall in that range. Also,

TABLE I. Values of D_0 and b obtained in this paper, compared with other references for other seismic zones. All values of D_0 are for hypocenters, except the Colombian data, which are for epicenters.

Country	D_0	b	Ref.
Chile	1.73, 2.02	0.9	
Colombia	1.61	0.57	[27]
Chile	2.1–2.2	1.2	[12]
India	1.65–1.85		[26]
Japan	1.9–2.9	0.6–1.5	[24]

the value of b can be related to the box-counting dimension [31] $b \simeq D_0/2$, which is also approximately satisfied by our results.

V. MULTIFRACTAL ANALYSIS

In this section, we will calculate the multifractal spectrum for our dataset [12–14]. In order to do so, we will use two methods of creating a grid for the data, either in two dimensions (for epicenters) and in three dimensions (for hypocenters). One method is histogram partitioning, in which case the geographical zone is divided in boxes (squares in two dimensions, cubes in three dimensions) of side ε, and $N_i(\varepsilon)$, the number of points inside each box i, is calculated. Thus, in this case the space is divided in nonoverlapping boxes. The second method is correlation-integral partitioning, and in this case $\tilde{N}_i(\varepsilon)$, the number of data points inside a ball (circle in two dimensions, sphere in three dimensions) of radius ε around each event x_i, excluding the point itself, is calculated. In this method, the space is divided in possibly overlapping balls of radius ε [32].

Both methods were applied to calculate the multifractal spectrum of epicenters and hypocenters data by first calculating the generalized Rényi entropy H_q [32]. For the histogram partitioning method

$$H_q = \frac{1}{1-q} \ln \left[\sum_i \left(\frac{N_i(\varepsilon)}{N} \right)^q \right], \tag{3}$$

where N is the total number of data points. For the correlation-integral partitioning method, on the other hand,

$$H_q = \frac{1}{1-q} \ln \left[\frac{1}{N} \sum_{i=1}^{N} \left(\frac{\tilde{N}_i(\varepsilon)}{N-1} \right)^{q-1} \right]. \tag{4}$$

Then, the Rényi multifractal spectrum is given by $D_q = \lim_{\varepsilon \to 0} -H_q(\varepsilon)/\ln(\varepsilon)$.

The strategy, then, first involves finding a range of values of ε where H_q scales linearly with ε. Then, from the slope of each curve, the value of D_q is determined. Finally the curves D_q vs q can be plotted, which is shown in Figs. 3(a) and 3(b), for epicenters and hypocenters, respectively. In principle, the range of ε for linear scaling depends on the value of q on the partitioning method, and on the dimension of the attractor (hypocenters and epicenters). However, for the seismic data used, it was found that, for $q > 0$, values of $\ln \varepsilon$ in the range $3 \leqslant \ln \varepsilon \leqslant 5$ were adequate for all methods and values of q for hypocenters, and that $3.6 \leqslant \ln \varepsilon \leqslant 5$ were adequate for epicenters. On the other hand, for epicenters and $q < 0$ [Fig. 3(a)], the range $4.2 \leqslant \ln \varepsilon \leqslant 5.2$ was used.

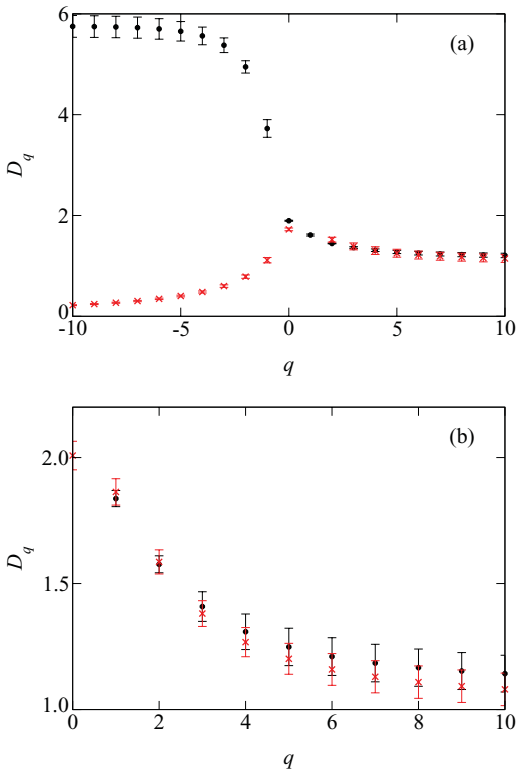

FIG. 3. (Color online) Rényi fractal dimension spectrum for (a) epicenters and (b) hypocenters. Red (gray) crosses: Histogram partitioning. Black circles: Correlation-integral partitioning. Error bars have been calculated from the error in calculating the slope which yields D_q.

In Fig. 3 the two methods explained above to calculate the Rényi fractal dimension spectrum are compared. For $q > 0$, both methods yield consistent results, however, as Fig. 3(a) shows, differences between methods can be huge for $q < 0$. In general, it is very difficult to get good results for $q < 0$ from experimental data, a problem which we will specifically address in Sec. VI.

It is worth noting that the values calculated for the multifractal dimensions are consistent with values for other seismic zones, where either only particular dimensions or the complete spectrum (for $q > 0$) have been obtained [13,14].

VI. MULTIFRACTAL SPECTRUM FOR $q < 0$

As noted in Sec. V, it is very difficult to get consistent results for the multifractal spectrum for experimental data, if $q < 0$. In order to do this, we take an analytical multifractal with adjustable parameters, which are chosen to fit the obtained multifractal spectrum for $q > 0$. Then, the spectrum for $q < 0$ is calculated for the analytical model. In our case, we will choose a generalized two-scale Cantor set [15,16]. The usual Cantor set can be obtained from an iterative process, where in each iteration a given segment is divided in three equal parts, and the middle part is discarded. Instead, we consider a set where the sum of the measures of the new segments is not necessarily the same as the measure of the previous segment

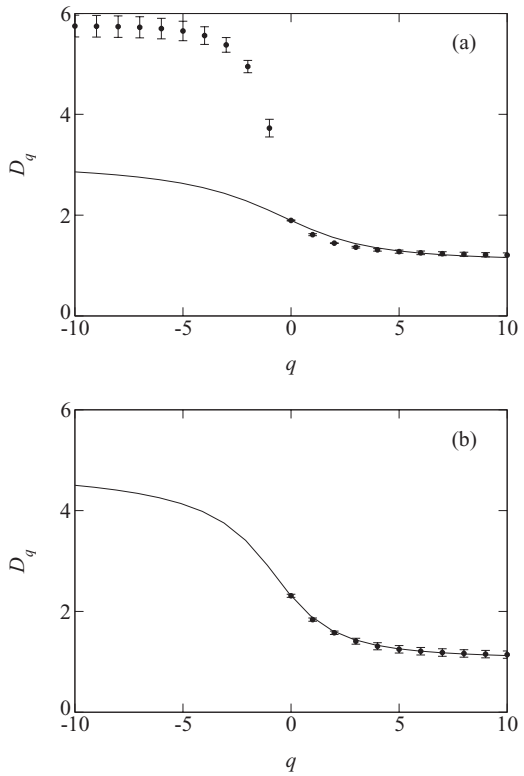

FIG. 4. Rényi fractal dimension spectrum for (a) epicenters and (b) hypocenters, extended to $q < 0$ by using an asymmetric, conservative Cantor-set model, Eq. (5).

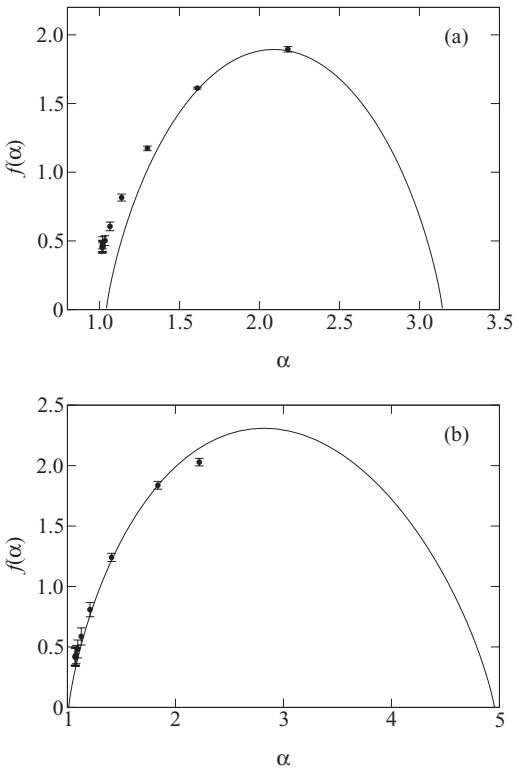

FIG. 5. Same as Fig. 4, but for the multifractal singularity spectrum. (a) Epicenters and (b) hypocenters, extended to $q < 0$ by using an asymmetric, conservative Cantor-set model, Eq. (5).

(this is given by two parameters p_1, p_2, where $p_1 + p_2 = 1$ corresponds to the usual, conservative case), and where the length of each new segment is not necessarily the same (this is given by two additional parameters, l_1 and l_2, where $l_1 = l_2$ corresponds to the usual, symmetric Cantor set). This model has been successfully used for an analysis similar to ours, but for solar wind data [17].

In the model, the multifractal dimension D_q turns out to satisfy the following equation:

$$p_1^q l_1^{(1-q)D_q} + p_2^q l_2^{(1-q)D_q} = 1. \quad (5)$$

Thus, the values of p_1, p_2, l_1, and l_2 which best fit the curve D_q vs q, for $q > 0$, are found which determines the Cantor set and its multifractal spectrum for all values of q.

Figure 4 shows the multifractal spectrum obtained with this method. The $q > 0$ region was fitted using data from the correlation-integral partitioning method which, as seen in Fig. 3(a), yields results which are more consistent with the expected form of the multifractal spectrum than with the histogram partitioning. The best fit for epicenters was obtained for a conservative, nonsymmetric Cantor set, given by $p \equiv p_1 = 1 - p_2 = 0.680, l_1 = 0.691$, and $l_2 = 0.696$. For hypocenters, the best fit corresponds to $p \equiv p_1 = 1 - p_2 = 0.675$, $l_1 = 0.6781$, and $l_2 = 0.797$. Notice, however, that the fit for hypocenters is better than for epicenters. This is more evident when calculating the multifractal singularity spectrum (see below).

Figure 5 shows the corresponding multifractal singularity spectrum (called the Mandelbrot fractal dimension spectrum in Ref. [32]), obtained from the results in Fig. 4 by the Legendre transform [15]

$$\alpha = \frac{\partial}{\partial q}[(q-1)D_q], \quad f(\alpha) = q\alpha - (q-1)D_q. \quad (6)$$

The fit of the $f(\alpha)$ function is much better for hypocenters than epicenters. This may be an indication that the multifractal generator can be improved. The generalized Cantor set was chosen because of its simplicity, and its good results for solar wind data as mentioned above. However, it is probably not adequate for every multifractal set. Thus, Fig. 5 shows that the Cantor set can still be a proper representation for seismic data, at least for hypocenters, although other generators should be considered as well. We plan to deal with this in the future.

VII. SUMMARY

A statistical and fractal analysis of seismic activity in the central zone of Chile has been carried out. The frequency of earthquakes as a function of magnitude follows the well-known Gutenberg-Richter power law, with a b value of -0.901. The self-similar structure of the data is also revealed by a fractal study of them. In effect, the box-counting dimension D_0 for epicenters and hypocenters was calculated. It is found that D_0 is not an integer, although fractality is more evident for epicenters ($D_0 = 1.73$).

Although the data analyzed cover a region 700 km in depth, 98% of the data have a depth above 150 km, thus they may be considered mostly shallow events. This suggests that, at least for these data, results obtained for epicenters may be more

representative of the crustal and upper mantle dynamics than for deep hypocenters.

The data also have a multifractal structure. Both the Rényi fractal dimension spectrum and the scaling index spectrum are calculated. Usually, only the region of the multifractal spectrum corresponding to the positive index of multifractal measure q is calculated, since it is the region which can be reliably calculated from experimental data. In this paper we have used a generalized Cantor-set model, parametrized to fit the $q > 0$ region, and then use it to calculate an extension of the spectrum for $q < 0$. Certainly, other multifractal set generators can be considered, but the Cantor-set model has the advantage of being particularly simple, and that it had been successfully used for a similar purpose, although in a very different system such as solar wind data.

It is interesting to note that the characteristic values calculated (b, D_0) lie within the range of calculated values for other seismic zones, revealing that these results hold regardless of the detailed structure of the plates and faults involved in the seismic activity. Thus, these results should contribute to a better understanding of the universal features of seismic activity.

ACKNOWLEDGMENTS

This project has been financially supported by FONDECyT under Contracts No. 1070854 and No. 1110135 (J.A.V.), No. 1080658 (V.M.), and No. 1090225 (J.R.). D.P. acknowledges financial support from CONICyT under Contract No. 21070671. We are thankful for financial support by Centro para el Desarrollo de la Nanociencia y la Nanotecnología, CEDENNA (J.A.V., V.M., and J.R.). We also thank the Chilean Servicio Sismológico Nacional for their generous collaboration by providing the data for this paper.

[1] S. Abe and N. Suzuki, Nonlinear Proc. Geophys. **13**, 145 (2006).
[2] G. Currenti, C. del Negro, V. Lapenna, and L. Telesca, Nat. Hazards Earth Syst. Sci. **5**, 555 (2005).
[3] K. Gotoh, M. Hayakawa, N. Smirnova, and K. Hattori, Phys. Chem. Earth **29**, 419 (2004).
[4] C. Papadimitriou, M. Kalimeri, and K. Eftaxias, Phys. Rev. E **7**, 036101 (2008).
[5] I. Zaliapin, A. Gabrielov, V. Keilis-Borok, and H. Wong, Phys. Rev. Lett. **101**, 018501 (2008).
[6] P. Bak, C. Tang, and K. Wiesenfeld, Phys. Rev. A **38**, 364 (1988).
[7] K. Bhattacharya and S. S. Manna, Physica A **384**, 15 (2007).
[8] J. X. de Carvalho and C. P. C. Prado, Phys. Rev. Lett. **84**, 4006 (2000).
[9] T. Chelidze and T. Matcharashvili, Tectonophysics **431**, 49 (2007).
[10] M. de Sousa Vieira, Phys. Rev. Lett. **82**, 201 (1999).
[11] D. Legrand, A. Calahorrano, B. Guillier, L. Rivera, M. Ruiz, D. Villagómez, and H. Yepes, Tectonophysics **344**, 15 (2002).
[12] D. Cernadas, A. Osella, and N. Sabbione, Pure Appl. Geophys. **152**, 57 (1998).
[13] P. P. Dimitriu, E. M. Scordilis, and V. G. Karacostas, Nat. Hazards **21**, 277 (2000).
[14] P. N. S. Roy and A. Padhi, Pure Appl. Geophys. **164**, 2271 (2007).
[15] T. C. Halsey, M. H. Jensen, L. P. Kadanoff, I. Procaccia, and B. I. Shraiman, Phys. Rev. A **33**, 1141 (1986).
[16] C. Meneveau and K. R. Sreenivasan, Phys. Rev. Lett. **59**, 1424 (1987).
[17] A. Szczepaniak and W. M. Macek, Nonlinear Proc. Geophys. **15**, 615 (2008).
[18] B. Gutenberg and C. F. Richter, *Seismicity of the Earth and Associated Phenomenon* (Princeton University Press, Princeton, NJ, 1954).
[19] http://ssn.dgf.uchile.cl/
[20] C. F. Richter, *Elementary Seismology* (Freeman, Princeton, NJ, 1958).
[21] X. Lei and K. Kusunose, Geophys. J. Int. **139**, 754 (1999).
[22] P. Mandal and B. K. Rastogi, Pure Appl. Geophys. **162**, 53 (2005).
[23] K. Nanjo and H. Nagahama, Chaos Solitons Fractals **19**, 387 (2004).
[24] K. Nanjo and H. Nagahama, Pure Appl. Geophys. **157**, 575 (2000).
[25] M. Sahimi, M. C. Robertson, and C. G. Sammis, Physica A **191**, 57 (1992).
[26] P. M. Bhattacharya, R. K. Majumdar, and J. R. Kayal, Curr. Sci. **82**, 1486 (2002).
[27] A. Caneva and V. Smirnov, Earth Sci. Res. J. **8**, 3 (2004).
[28] M. Sahimi, M. C. Robertson, and C. G. Sammis, Phys. Rev. Lett. **70**, 2186 (1993).
[29] M. C. Robertson, C. G. Sammis, M. Sahimi, and A. J. Martin, J. Geophys. Res. B **100**, 609 (1995).
[30] C. Frohlich and S. D. Davis, J. Geophys. Res. B **98**, 631 (1993).
[31] K. Aki, in *Earthquake Prediction: An International Review*, Vol. 4 of Maurice Ewing Series, edited by D. W. Simpson and P. G. Richards (AGU, Washington, DC, 1981), pp. 566–574.
[32] M. Potter and W. Kinsner, in *ICASSP (IEEE International Conference on Acoustics, Speech and Signal Processing) 2007, Honolulu*, Vol. 3 (IEEE, New York, 2007), pp. III 989–III 992.